Inhomogeneous broadening of intersubband transitions in $In_{0.45}Ga_{0.55}As/Al_{0.45}Ga_{0.55}As$ multiple quantum wells

G. Beadie and W. S. Rabinovich
Code 5642, Naval Research Laboratory, Washington, D.C. 20375-5320

D. S. Katzer
Code 6850, Naval Research Laboratory, Washington, D.C. 20375-5320

M. Goldenberg
SFA, Inc., Largo, Maryland 20774-5322
(Received 16 September 1996)

The contributions of homogeneous and inhomogeneous broadening mechanisms to the linewidth of an intersubband transition in an $In_{0.45}Ga_{0.55}As/Al_{0.45}Ga_{0.55}As$ multiple quantum well are determined by line-shape fitting and saturation intensity spectroscopy. An intersubband transition at 327 meV is found with a total linewidth of 36 meV and an underlying homogeneous linewidth of 14 meV. The sizes of various sources of inhomogeneous broadening are estimated and the implications for intersubband nonlinear optics are discussed. [S0163-1829(97)05715-9]

I. INTRODUCTION

Intersubband transitions in quantum wells have been the subject of intense study over the past few years, both as testbed systems for aspects of quantum mechanics and solid-state theory as well as for possible applications to infrared detectors,[1] nonlinear optical devices,[2–7] modulators,[8] and lasers.[9] Because of the ability to grow specified potential structures using molecular-beam epitaxy and other techniques it has been possible to engineer ''artificial molecules'' with mid-infrared resonances.

Both the linear and nonlinear optical properties of these systems have, in general, been well described by effective mass theory with some additional corrections for many-body effects.[10,11] In this framework, intersubband nonlinear optical properties have been modeled in terms of a set of degenerate multilevel systems. An important material parameter for these models is T_2, the dephasing time between subbands. When calculating the expected nonlinearity of an intersubband system, some authors have assumed that the broadening mechanism is homogeneous and hence that T_2 is simply inversely proportional to the full width at half maximum of the measured intersubband absorption. For nonlinearities in the long-wavelength region, near 10 μm, this approximation may be valid. Several measurements of good-quality $GaAs/Al_xGa_{1-x}As$ multiple quantum wells at these wavelengths have shown that the intersubband transition is homogeneously broadened, fitting well to a Lorentzian line shape with a linewidth of 3–10 meV.[12–15]

There is, however, a great deal of practical interest in shorter-wavelength intersubband transitions of 5 μm or less. Applications for such transitions include frequency conversion[16,17] and χ^3 effects[7] using either mid-infrared laser diodes or other available near-infrared sources such as holmium, thulium, or erbium solid-state lasers. Short-wavelength intersubband transitions generally require higher conduction-band offsets than those available within the $GaAs/Al_xGa_{1-x}As$ system. For example, using the larger offsets provided by the $In_xGa_{1-x}As/In_xAl_{1-x}As$ (Ref. 18) and $In_xGa_{1-x}As/Al_xGa_{1-x}As$ (Refs. 19 and 20) systems, transitions with wavelengths down to 2 μm have been observed. Generally, however, the shorter wavelengths are accompanied by larger intersubband linewidths. In good quality, *n*-type, multiple quantum wells, observed linewidths are approximately 10% of the intersubband energy.

The increase in linewidth is important because it results in the reduction of the resonant nonlinear susceptibility of these materials. However, the amount of this reduction, and the way the nonlinearity saturates at high intensity, depends on whether the source of this broadening is homogeneous or inhomogeneous; i.e., whether each region of the quantum well, both laterally and vertically, has an intersubband transition with the same central energy or whether different regions have different central energies. In the former case, the linewidth is due entirely to dephasing, and T_2 can legitimately be related to the inverse of the linewidth. In the latter case, there is an underlying homogeneous linewidth that must be separated from the inhomogeneous linewidth before T_2 can be determined.

The effect of inhomogeneous broadening on excitonic transitions in quantum wells has been examined by several workers. In general, inhomogeneous broadening has been found to be an important effect and has been attributed to a variety of sources including well-width fluctuations,[21,22] inhomogeneous strain,[23] and alloy clustering.[24]

There has been much less work reported on the study of inhomogeneous broadening of intersubband transitions.[12] While many broadening mechanisms are shared between excitonic transitions and intersubband transitions, there are some significant differences. Intersubband broadening involves the energy levels of just one carrier type, but involves higher subbands. In addition, there are other broadening mechanisms such as the effects of impurity doping. In this paper we model some of the effects of material disorder on

intersubband transitions and experimentally determine the degree of inhomogeneous broadening in a strained $In_xGa_{1-x}As/Al_xGa_{1-x}As$ multiple quantum well sample that exhibits a short-wavelength (3.75 μm) intersubband transition. The homogeneous and inhomogeneous linewidths are determined by two independent techniques: line-shape fitting and saturation intensity spectroscopy.

II. SAMPLE PREPARATION

The sample we examined was grown by molecular-beam epitaxy and consisted of 50 periods of a structure with a 40-Å $In_{0.45}Ga_{0.55}As$ well and an 80-Å $Al_{0.45}Ga_{0.55}As$ barrier. The wells were uniformly doped with silicon to a sheet carrier concentration of $6.6\times10^{11}/cm^2$ as determined by the integrated absorption fraction of the intersubband transition. $In_{0.45}Ga_{0.55}As$ is highly lattice mismatched to $Al_{0.45}Ga_{0.55}As$. To compensate for this mismatch the multiple quantum well (MQW) was grown on a linearly graded buffer.[20,25] The substrate was semi-insulating 001 GaAs. The buffer was graded from GaAs to $In_{0.25}Ga_{0.75}As$ with a 15%/μm grade. The final indium fraction of the buffer was somewhat larger than the average of the MQW.[20] Because of residual strain in the buffer[26] this produces a better match to the average lattice constant of the MQW. The substrate growth temperature was kept constant at 400 °C for both the buffer and multiple quantum well growth. The surface of the quantum well was smooth and specular to the naked eye. Similar samples grown with a buffer linearly graded to 30% indium showed much rougher, cloudy surfaces and had intersubband linewidths approximately twice as broad.

The intersubband absorption was measured in a Fourier transform infrared (FTIR) spectrometer with p-polarized light at Brewster's angle. In order to increase the absorption length of the intersubband transition for the saturation measurements, we cleaved three pieces of the wafer and formed a stack. Without care, this can cause a form of inhomogeneous broadening due to radial variations in the growth rate of the wafer. To avoid this problem all three pieces were cleaved from sections of the wafer equidistant from the center. Separate FTIR spectra of each piece showed that they had the same shape and full width at half maximum (FWHM). Their peaks differed in energy by less than 1 meV. The spectrum of the stack showed no etalon fringing at Brewster's angle. The spectrum is shown in Fig. 1.

The central energy of the intersubband transition is at 328 meV with a FWHM of 36 meV. The relative linewidth of 11% is on par with the best reported in these materials[20] and is indicative of the high quality of the sample.

III. MODELING OF THE BROADENING OF THE INTERSUBBAND TRANSITION

The intersubband linewidth is determined by many factors, some of which act to homogeneously broaden the line, such as phonon and impurity scattering, and some of which act to inhomogeneously broaden it. As with excitonic broadening, many of the mechanisms can contribute homogeneous or inhomogeneous broadening depending on their scale and the degree of localization of the carriers. For example, small-scale fluctuations in the well width homogeneously broaden

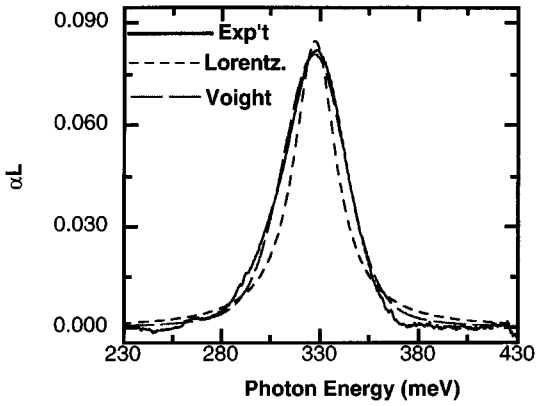

FIG. 1. Experimental (Expt) absorption spectrum of the quantum well sample using p-polarized light at Brewster's angle, along with best fits to a Lorentzian (Lorentz.) and Voight line shape.

the line whereas larger-scale island formation or well-to-well fluctuations inhomogeneously broaden it. While the exact nature of the intersubband broadening will depend on the structure and growth conditions of the sample, we can reasonably estimate the possible sizes of various contributions by modeling the effects of various material parameters upon the intersubband energy levels.

Towards this end, we solved for the energy levels and wave functions of the MQW, including many-body effects, using a self-consistent transfer matrix code. Nonparabolicity was accounted for using an energy-dependent effective mass.[27] The effects of the Hartree and exchange potentials were added to the structural potential of the quantum wells and carriers.[10,11]

The net Hamiltonian of the system in this approximation is

$$\left\{\frac{-\hbar^2\partial^2}{2m^*(z)\partial z^2}+V_{\mathrm{QW}}(z)+V_H(z)+V_{\mathrm{xc}}(z)\right\}\Psi_i=E\Psi_i, \tag{1}$$

where z is the coordinate perpendicular to the plane of the quantum wells, $m^*(z)$ is the in-plane effective mass, $V_{\mathrm{QW}}(z)$ is the structural potential of the quantum well, $V_H(z)$ is the Hartree potential, $V_{\mathrm{xc}}(z)$ is the exchange-correlation potential, and Ψ_i is the envelope wave function.

The Hartree potential is determined by solving Poisson's equation

$$V_H(z)=\frac{e}{\epsilon\epsilon_0}\int_{-\infty}^{z}(z-z')\rho(z')dz', \tag{2}$$

where e is the electronic charge, ϵ is the relative permittivity, ϵ_0 is the permittivity in vacuum, and $\rho(z)$ is the charge density which can be expressed as

$$\rho(z)=e[N_D(z)-n(z)], \tag{3}$$

where

$$n(z)=\sum_i n_i^{2d}|\Psi_i(z)|^2,$$

n_i^{2d} is the sheet density for each sublevel, and $N_D(z)$ is the dopant ion density.

The exchange-correlation potential is approximated in the local-density approximation using the interpolation scheme of Hedin and Lundquist.[28] Then the potential is

$$\phi_{\rm xc}(z) = -\left[1 + \frac{0.7734 r_s}{21} \ln\left(1 + \frac{21}{r_s}\right)\right]\left[\frac{2}{\pi\alpha r_s}\right] Ry^*, \quad (4)$$

where

$$r_s = \frac{1}{a^* \sqrt[3]{4\pi n(z)/3}}, \quad a^* = \frac{4\pi\epsilon\hbar^2}{m^* e^2},$$

$$\alpha = \sqrt[3]{4/9\pi}, \quad Ry^* = \frac{e^2}{8\pi\epsilon a^*}.$$

Because $In_xGa_{1-x}As$ and $Al_xGa_{1-x}As$ are not lattice matched, the effects of strain must be taken into account. This is done by first choosing an average lattice constant for the whole quantum well structure as determined by the linearly graded buffer. This lattice constant, along with the parameters and theory described by Arent *et al.*,[29] are then used to calculate the effects of strain on the band gaps. A strain-dependent effective mass determined from cyclotron resonance measurements of $In_xGa_{1-x}As/Al_xGa_{1-x}As$ pseudomorphic structures[30] was also included.

Because several of the terms in Eq. (1) depend upon the wave functions of the carriers, a self-consistent solution must be obtained by iterative means. We began by setting the contributions of the Hartree and exchange-correlation potentials to zero. The wave functions of the subbands were then determined using the transfer matrix method. The Hartree and exchange-correlation potential were calculated using these wave functions and added to the potential. The solution was iterated until the energy levels changed by less than 0.1 meV.

The intersubband transition energy can also be shifted by depolarization and excitonlike effects. We calculate these shifts using the formulation of Ando.[31] The intersubband transition energy is shifted to

$$\tilde{E}_{ij}^{\,2} = E_{ij}^2 (1 + a_{ij} - b_{ij}), \quad (5)$$

where $E_{ij} = E_i - E_j$ is the intersubband transition energy given by the solution of Eq. (1). a_{ij} accounts for the depolarization shift and is given by

$$a_{ij} = \frac{2e^2 (n_j^{2D} - n_i^{2D}) S_{ij}}{\epsilon\epsilon_0 E_{ij}}, \quad (6)$$

where

$$S_{ij} = \int_{-\infty}^{\infty} dz \left(\int_{-\infty}^{z} dz' \Psi_i(z') \Psi_j(z') \right)^2$$

and b_{ij} accounts for the excitonlike shift and is given by

$$b_{ij} = \frac{-2(n_j^{2D} - n_i^{2D})}{E_{ij}} \int_{-\infty}^{\infty} dz \; \Psi_i^2 \Psi_j^2 \frac{\partial \phi_{\rm xc}}{\partial n(z)}. \quad (7)$$

Finally, relaxation times between intersubband levels were calculated based upon LO phonon scattering using the calculated wave functions.

We applied this model to the structure described in Sec. II. For the specified growth parameters the model predicts an energy of 335 meV for the level 1 to level 2 intersubband transition, quite close to the measured value of 328 meV. The dipole moment for this transition is 1.1 nm. The good agreement between the model and sample indicate that the most important effects determining the intersubband energy have been taken into account.

Using this model, we considered some of the most likely sources of broadening. One of the most widely studied broadening mechanisms for excitonic states is well-width fluctuation. These generally consist of monolayer shifts about the design thickness and may occur from one well to the next, or laterally through the formation of islands. For the intersubband structure described above, these are also one of the largest potential contributors to the intersubband linewidth. For a (-1) monolayer change in well width we calculate a shift in the intersubband energy of 19.7 meV, while for a $(+1)$ monolayer shift we calculate a change in energy of -19.0 meV. Gammon, Shannabrook, and Katzer performed spatially resolved studies of excitonic line broadening by well-width variations and showed that the energy shift could be either discrete, corresponding to integer monolayer changes in well width, or continuous, depending upon the size of the islands.[22] Thus these fluctuations may produce a spectrum composed of well-resolved peaks or, as we observe, a single broad peak. The sizes of the energy shifts due to well-width fluctuations are suggestive, since they correspond closely to the total linewidth seen in the spectrum. Fluctuations of more than ± 1 monolayer seem unlikely in this sample since they would produce approximately twice the linewidth observed (though they may explain the large linewidth seen in samples grown with nonoptimal buffers). The importance of well-width fluctuations is not surprising in the narrow wells needed to produce short-wavelength intersubband transitions. Weisbuch *et al.* predicted a $1/L^3$ dependence of linewidths based upon an infinite square well model.[32] In actual systems, the dependence on well width is not as strong due to the effects of nonparabolicity and because of the finite barrier height.

While well-width variations are probably the dominant broadening mechanism, several other effects can contribute to the linewidth. High-indium content $In_xGa_{1-x}As/Al_xGa_{1-x}As$ quantum wells allow very short-wavelength intersubband transitions because of their large conduction-band offset. However, this is achieved at the cost of strain in the $In_xGa_{1-x}As$ and $Al_xGa_{1-x}As$ layers. While using a graded buffer helps a great deal in material quality, the effects of lateral or well-to-well inhomogeneous strain may still broaden the line. The largest effect of strain on the intersubband energy comes from changes in the effective mass of the electron through shifts in the band gaps of the materials. We assume, in our model, that the effective mass of the strained material can be related to that of the unstrained material by[30]

$$m_{\rm st}^* = m\left(1 + \frac{\Delta E_g}{E_g}\right), \quad (8)$$

where m_{st}^* is the strained effective mass, E_g is the unstrained band gap, and ΔE_g is the shift in the band gap introduced by strain.

Raman studies of $In_{0.17}Ga_{0.83}As/GaAs$ quantum wells grown on GaAs have shown that lateral strain islands form with a size of about 30 μm.[23] Similar studies have not yet been performed on high-indium $In_xGa_{1-x}As/Al_xGa_{1-x}As$ structures grown on graded buffers. As mentioned above, calculations of transition energies require an estimate of the lattice constant. To estimate the maximum possible energy shift due to inhomogeneous strain, this lattice constant was allowed to vary between the two extremes of that of GaAs to that of $In_{0.45}Ga_{0.55}As$. The maximum total shift in intersubband energy predicted by our model is then 21 meV.

Because we use ternary alloys for both our well and barrier material, statistical variation, as well as long term drift, of the alloy concentration must be considered. Singh and Bajaj have studied this problem for excitonic line broadening.[24] They showed that the exciton is affected by a statistical fluctuation of the composition of the alloy that depends upon the volume of the exciton and the cluster size of the alloy. Studies of alloy disorder in $In_{0.5}Ga_{0.5}As$ by Dimoulas *et al.* have shown a cluster size of about 10 Å.[33] To estimate the fluctuations in the composition of the well alloy we need to specify a sensing volume for the electron. This is a complex problem, but for a crude estimate we assume a size in the z dimension defined by the well width and in the transverse dimension by the mean free path of the electron (about 400 Å). This predicts a fluctuation of x, the indium content, of $\pm 2\%$, which yields a shift in intersubband energy of about 6 meV. Alloy fluctuations of the aluminum content of the barriers have a similar magnitude and a somewhat smaller effect on the intersubband energy. In addition to statistical fluctuations, long term drift of the growth rates, particularly of the aluminum, may produce well-to-well changes in alloy composition, but this effect is harder to quantify and will depend on the individual molecular-beam epitaxy (MBE) machine.

Finally, we consider band nonparabolicity as an inhomogeneous broadening mechanism. Because the dispersions in the first and second subbands are different, the separation of the subbands becomes a function of k_T, the transverse momentum. In a simple, single-electron picture, this effect would cause a broadening of the intersubband transition in our sample of about 10 meV. However, unlike all the other broadening mechanisms we have discussed, band nonparabolicity is inherently a many-body effect. Experimental and theoretical investigations of inhomogeneous broadening due to nonparabolicity suggest that the single-electron picture significantly overestimates the size of the effect. Von Allmen, in a many-body calculation of nonparabolicity broadening, showed a reduction by a factor of 5 over the single-electron calculation.[12] This is borne out by experiment. Several experimental studies of the linewidths of intersubband transitions in heavily doped $GaAs/Al_xGa_{1-x}As$ quantum wells have shown total linewidths near to or smaller than the linewidth contribution of nonparabolicity in the single-electron picture[13,14] alone. We have also seen empirical evidence that nonparabolicity is overestimated in the single-electron picture. Single-electron nonparabolicity broadening should produce a line with a very strong asymmetry on the low-energy side, which is not seen in our sample. In addition, a sample identical in structure to that described in Sec. II, but with half the doping, showed the same linewidth, whereas a single-electron picture of nonparabolicity broadening would predict a drop in linewidth. Other, very heavily doped, $In_xGa_{1-x}As/Al_xGa_{1-x}As$ quantum wells that we have grown have shown *total* linewidths smaller than the single-electron nonparabolicity broadening. In sum, we conclude that nonparabolicity is probably dominated by other broadening mechanisms, such as well-width fluctuations, in our sample.

To conclude this section, we note that most of the inhomogeneous broadening mechanisms described above cause shifts in the subband levels that are proportional to the energy of these levels, consistent with the rule of thumb that the intersubband linewidth in good-quality material is about 10% of the energy.

IV. LINE-SHAPE FITTING

Spectroscopy and saturation intensity studies of good-quality $GaAs/Al_xGa_{1-x}As$ quantum wells with intersubband transitions near 10 μm have shown them to be homogeneously broadened with linewidths between 3 and 10 meV depending on temperature and doping profile.[15,34,13,35,36] The line shapes of the intersubband transitions in these materials are well fit by a Lorentzian. Thus, as a starting point for approximating the effect of inhomogeneous broadening, we begin with a Lorentzian line shape. Figure 1 shows the measured spectrum of our sample as well as a Lorentzian fit to the spectrum. A nonlinear least-squares fitting algorithm was used and the peak location and linewidth were allowed to vary with the constraint that the integrated absorption fraction was equal to the experimental curve. As can be seen, the Lorentzian gives a poor fit, characteristic of a line that is inhomogeneously broadened: the peak is overestimated and the linewidth is underestimated. The Lorentzian fit is strongly rejected by χ^2 analysis.

The broadening mechanisms described above arise from random material fluctuations and are for the most part uncorrelated with each other. This sort of broadening is in general well described by a Voight profile: the convolution of a Gaussian with a Lorentzian. In gas spectroscopy Voight profiles are often used to describe lines that are Doppler broadened.[37] In addition, Kaushik and Hagelstein have used Voight profiles to describe the exciton line shape in quantum wells.[38]

The absorption due to a line with a Voight profile can be described by

$$\alpha_V(E)=\left(\frac{4\ln 2}{\pi\Gamma_I}\right)^{1/2}\int_{-\infty}^{\infty}\exp\left[(-4\ln 2)^2\left(\frac{E'-E_c}{\Gamma_I}\right)^2\right]\times\alpha_H g_H(E,E')dE', \tag{9}$$

where the homogeneous line-shape function is

$$g_H(E,E')=\left[\frac{\Gamma_H^2}{4[(E-E')^2+(\Gamma_H/2)^2]}\right], \tag{10}$$

Γ_I is the inhomogeneous linewidth, E_c is the center frequency of the inhomogeneous distribution, α_H is the absorp-

tion coefficient of the underlying homogeneous line shape, and Γ_H is the homogeneous linewidth.

We fit the spectrum of our sample using a Voight profile to determine the underlying homogeneous and inhomogeneous linewidths. The best fit was for a Γ_H of 11.5 meV and a Γ_I of 32 meV. As can be seen in Fig. 1 the fit is quite good. Acceptable fits (as determined by the variation of χ^2) could be obtained for values of Γ_H between 9 and 14 meV. This value of homogeneous linewidth is consistent with intersubband transitions at 10 μm in well-doped GaAs/$Al_xGa_{1-x}As$ samples at room temperature. It is three times smaller than the total linewidth of the intersubband transition in our sample, 36 meV. Thus line-shape analysis indicates that the sample is heavily inhomogeneously broadened.

V. INHOMOGENEOUS SATURATION THEORY

While detailed line-shape fitting is a powerful technique for determining the homogeneous and inhomogeneous linewidths of a transition, it is desirable to have an independent alternative technique. A widely used approach for gases[39] and some solids[40] is hole burning spectroscopy. This technique requires a tunable source and a fixed source or, for Doppler-broadened lines, a tunable source that is split into counterpropagating beams.

When only one tunable source is available, an alternative to standard hole burning spectroscopy is to measure the wavelength dependence of the saturation intensity. In a homogeneously broadened two-level system the absorption saturates as

$$\alpha(E,I)=\frac{\alpha_H g_H(E,E_0)}{1+I/I_{SH}(E,E_0)}, \tag{11}$$

where E is the photon energy, E_0 is the central energy of the transition, and I is the laser intensity. I_{SH} is the homogeneous saturation intensity defined by

$$I_{SH}=\frac{\epsilon_0 nhc\Gamma_H}{8\pi\mu^2\tau g_H(E,E_0)}, \tag{12}$$

where μ is the effective dipole moment of the transition (including any polarization coupling), τ is the relaxation time for the excitation, n is the index of refraction, h is Planck's constant, and c is the speed of light.

In a homogeneously broadened system, the saturation intensity as a function of photon energy varies as $g_H(E,E_0)^{-1}$, increasing as one moves away from line center. In a completely inhomogeneously broadened system, where the inhomogeneous linewidth is much larger than the homogeneous, the system saturates as $\alpha_0/\sqrt{1+I/I_{SI}}$, where I_{SI} is a constant, and the saturation intensity is independent of photon energy.

In an intermediate case, again assuming a Gaussian distribution for the inhomogeneous broadening, we must numerically integrate Eq. (11). The expression for the saturated absorption in the intermediate case is

$$\alpha_{\text{in hom}}(E,I)=\left(\frac{4\ln 2}{\pi\Gamma_I}\right)^{1/2}\int_{-\infty}^{\infty}\exp\left[(-4\ln 2)^2\left(\frac{E'-E_c}{\Gamma_I}\right)^2\right]\times\left[\frac{\alpha_H g_H(E,E')}{1+I/I_{SH}(E,E')}\right]dE'. \tag{13}$$

By measuring the saturation intensity of an absorption feature as a function of the photon energy we can determine the homogeneous and inhomogeneous linewidths. This technique is distinct from line-shape fitting and thus provides an independent measure of the linewidths.

The use of Eq. (11) or Eq. (13) to fit the saturation of an intersubband transition amounts to approximating the quantum well as a set of degenerate two-level systems. This approach has been used successfully in numerous saturation experiments on homogeneously broadened intersubband transitions.[34,36,41] In addition, a detailed Monte Carlo simulation of intersubband relaxation by Newson and Kurobe,[42] including the effects of intersubband, intrasubband, and intervalley relaxation, showed that the steady-state saturation of the absorption was very well described by a two-level homogeneous saturation expression.

Deviations from the two-level model can occur if the change in the population of the subbands significantly alters the energy difference or matrix elements between the subbands. This can arise from changes in the Hartree potential due to the different spatial distributions of the carriers in the subbands or due to a decrease in the depolarization shift.[43]

Using the model described in Sec. III, we calculated the changes in the intersubband energy due to laser excitation. At the saturation intensity we found the shift to be negligible (less than 1 meV). The energy shift is small because Stark effects due to changes in the Hartree terms are small in square, well-doped, quantum wells. Shifts due to the depolarization and excitonlike effects are also reduced compared to wider quantum wells because of the smaller overlap of the ground- and excited-state wave functions. Thus we conclude that Eq. (13) should be a good model for saturation of an inhomogeneously broadened intersubband transition.

VI. INHOMOGENEOUS SATURATION EXPERIMENT

To measure the saturation intensity of our sample as a function of photon energy we performed the following experiment. A $KTiOPO_4$ (KTP) optical parametric oscillator (OPO) pumped with the 1.06-μm line of a Q-switched Nd:YAG (YAG denotes yttrium aluminum garnet) laser was used to provide a strong, tunable mid-infrared laser pulse. The orthogonally polarized signal and idler beams from the OPO were separated using a set of ZnSe plates set at Brewster's angle. The mid-infrared idler beam from the OPO was then spatially filtered to ensure good mode quality. The idler beam was split into two parts. The first was sent to a pyroelectric detector placed before the sample. The rest of the beam was focused onto the sample. After transmission, a second, matched, pyroelectric detector measured the transmitted energy. Both detectors were connected to a ratiometer that exhibited a precision of $\pm 0.1\%$. We tuned the OPO to six photon energies that overlapped the intersubband absorption feature shown in Fig. 1. At each photon energy the transmission of the sample was measured as a function of

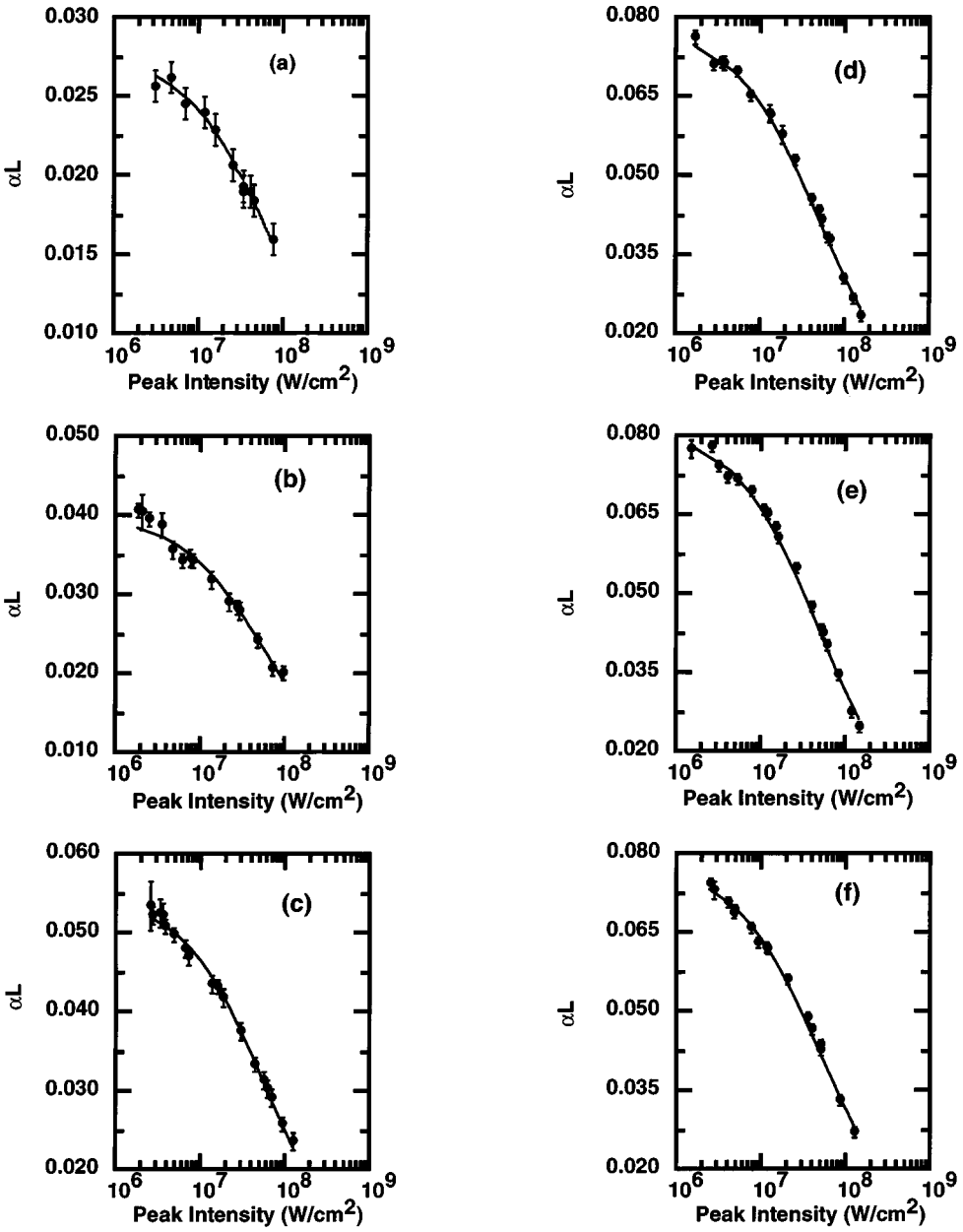

FIG. 2. Measured saturated absorption versus peak laser intensity and best fit at several photon energies. (a) 353 meV. (b) 348 meV. (c) 342 meV. (d) 336 meV. (e) 327 meV. (f) 323 meV.

incident power. The transmission was determined by averaging 100 shots from the OPO using the ratiometer. Three transmission measurements were taken at each power to determine the experimental error. The spatial profile of the beam was determined at each photon energy using a 128 $\times$128 pyroelectric camera and beam profiling software. The beam was slightly elliptical with a horizontal diameter of 470 μm, a vertical diameter of 580 μm, and a Raleigh length of about 2 cm. The temporal profile of the beam was also measured at each photon energy. The approximately Gaussian pulse envelope had a width of 5 ns.

Because the OPO did not operate on a single longitudinal mode, it was also necessary to determine the underlying fast time structure of the pulse that arose due to beating of the longitudinal modes. It is well known from nonlinear frequency conversion studies that a multimode laser source can act as if it has an effectively higher intensity than that determined by its pulse envelope.[44] We measured this statistical enhancement of the intensity directly, by doubling the signal beam of the OPO and measuring the spiking on a streak camera. We then numerically integrated Eq. (13) to determine the enhancement of the intensity.

The saturated absorption-length product as a function of peak OPO intensity for each of the photon energies is shown in Figs. 2(a)–2(f). We performed a nonlinear least-squares fit of Eq. (13) integrated over the measured spatial and temporal profiles of the beam. In fitting the data, the value of α_H was determined by the FTIR absorption spectra and the value of μ was determined by the transfer matrix model of the structure. We used the following procedure to determine the best values for Γ_H and Γ_I: We fixed a value of Γ_H and then fit the FTIR absorption spectrum with the Voight profile, Eq. (9), to

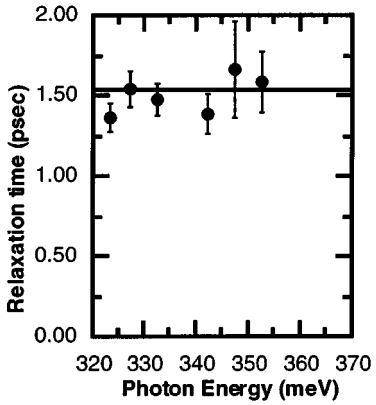

FIG. 3. The value of τ, the intersubband relaxation time versus photon energy, as determined by the fit of the saturation curves, compared to the theoretical value (horizontal line).

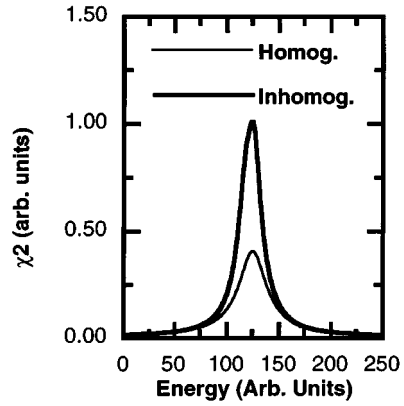

FIG. 5. Theoretical value of χ^2 for an inhomogeneously and homogeneously broadened system.

determine the value of Γ_I that best matched the spectrum. Using a range of values for Γ_H between 6 and 18 meV we produced a set of Γ_H-Γ_I pairs. We then used these pairs in Eq. (13) and fit the saturated absorption data for each photon energy with τ, the intersubband relaxation time, as the fitting parameter. When using the correct choice of Γ_H-Γ_I pair the fitted value of τ should be the same, within experimental error, for all values of photon energy. The error in the fits was determined by Monte Carlo resampling and fitting of the data.[45] We found that a Γ_H-Γ_I pair of 14–29.9 meV gave the best results. The fitted value of τ as a function of photon energy is shown in Fig. 3 along with the theoretical value, assuming LO phonon scattering, of about 1.5 ps. For values of Γ_H between 10 and 16 meV most though not all of the fitted values of τ were within experimental error of each other, so this range represents the uncertainty in our measurement.

To further illustrate the difference between the saturation that we observe and that expected in a homogeneously broadened system we compare the dependence of saturation intensity on photon energy. For a homogeneously broadened system the absorption drops to half its small signal value at the saturation intensity. An inhomogeneously broadened system has a different functional dependence, but we can define an effective saturation intensity as that intensity at which the absorption is half its small signal value. In Fig. 4 we show the ratio of the saturation intensity at a given photon energy to that at line center. Both the experimental and theoretical values are shown. The two theoretical curves correspond, respectively, to a homogeneously broadened system with a linewidth of 36 meV, and to an inhomogeneously broadened system with a homogeneous linewidth of 14 meV and an inhomogeneous linewidth of 29.9 meV. Clearly the system is much better described by the inhomogeneous curve.

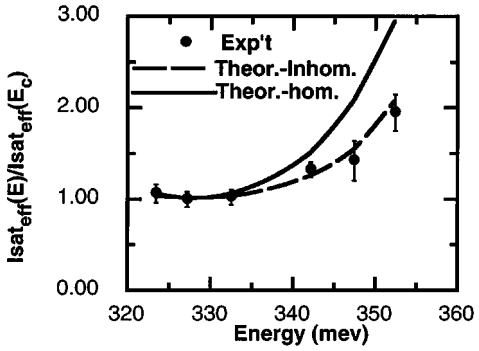

FIG. 4. Measured effective saturation intensity versus photon energy compared to theoretical calculations assuming a homogeneously and inhomogeneously broadened system.

VII. DISCUSSION

Both line-shape fitting and saturation intensity measurements on our sample agree, to within experimental error, that the homogeneous linewidth of the sample is 11–14 meV, about one-third of the total linewidth of the transition. The good agreement between the two methods is important not only as additional confirmation, but also because it indicates that line-shape fitting alone should be a reliable method of determining the underlying homogeneous linewidth. Line-shape fitting is a much simpler technique than saturation intensity measurements and does not require a strong tunable source.

In addition to contributing to the fundamental understanding of broadening mechanisms for intersubband transitions, the degree of inhomogeneous broadening is of importance for applications which make use of the nonlinear optical properties of intersubband transitions. For the same value of FWHM, the nonlinear susceptibility of a resonant system that is inhomogeneously broadened may be larger than that of a system that is homogeneously broadened. This is displayed in Fig. 5, which shows theoretical calculations of χ^2 for two doubly resonant intersubband systems.[3] For the calculation, we assumed that one system was homogeneously broadened on both transitions and that the other system was inhomogeneously broadened on both transitions. For the inhomogeneous case we assume a total linewidth equal to the homogeneous case with an underlying homogeneous linewidth that is half the total linewidth. As can be seen, the χ^2 of the inhomogeneous system is two and a half times as large at resonance. We also assumed that the inhomogeneous broadening on both transitions was anticorrelated. That is, that a material fluctuation shifted the transitions in opposite directions. For real systems the correlation will be more complex.

In addition to the effect of inhomogeneous broadening on the size of the nonlinearity, there will be an effect upon the saturation of the conversion efficiency. Several theoretical treatments of the optimal conditions for frequency conversion efficiency using intersubband systems have considered the effects of saturation to determine the optimal detunings of the fields from resonance.[46,47] These treatments have assumed that the system saturates homogeneously. Since they have been applied to the problem of doubling the frequency of 10-μm radiation, this is probably a valid assumption. However, these calculations will not apply to a system that is inhomogeneously broadened, for example to the problem of difference frequency generation using short-wavelength intersubband transitions.[17] The inhomogeneous system will saturate more slowly, increasing the conversion efficiency. On the other hand, detuning from resonance will have less advantage since the saturation intensity does not go up as rapidly away from line center. Experimental measurements, and a theoretical model, of the effects of inhomogeneous broadening on intersubband frequency conversion, performed in our laboratory, will be published elsewhere.

The strong dependence of nonlinear optical properties of intersubband transitions on the *nature* of the broadening indicates that material systems should be evaluated based upon line-shape fitting rather than simple measures of the full width at half maximum. In particular, techniques such as growth interrupts, which can change the roughness spectrum of interfaces, or barrier doping may not appreciably change the *total* linewidth of a system but may change the apportionment of that linewidth between inhomogeneous and homogeneous mechanisms and significantly affect the nonlinear susceptibility.

VIII. CONCLUSION

We have determined the underlying homogeneous linewidth of a short-wavelength intersubband transition in a strained $In_xGa_{1-x}As/Al_xGa_{1-x}As$ quantum well. The transition, at an energy of 328 meV, had a total linewidth of 36 meV and a homogeneous linewidth of between 11 and 14 meV. Both line-shape fitting and saturation intensity spectroscopy agree to within experimental error. The $In_xGa_{1-x}As/Al_xGa_{1-x}As$ material system is of technological importance because it has produced the narrowest linewidth, short-wavelength intersubband transitions, so these results have practical significance. In addition, we expect that many of the features and broadening mechanisms we have found will be present in other systems that display short-wavelength intersubband transitions as well. While strain may not occur in all systems, the effects of well-width variations will always be present.

ACKNOWLEDGMENTS

The authors acknowledge the support of the Office of Naval Research. One of us, G.B., acknowledges support from NRL-NRC.

[1] B. F. Levine, K. K. Choi, C. G. Bethea, J. Walker, and R. J. Malik, Appl. Phys. Lett. **50**, 1092 (1987).
[2] M. K. Gurnick and T. A. DeTemple, IEEE J. Quantum Electron. **19**, 791 (1983).
[3] Jacob B. Khurgin, *Second Order Intersubband Nonlinear Optical Susceptibilities of Asymmetric Quantum Well Structures* (Optical Society of America, Washington, DC, 1989), pp. 1–69.
[4] M. M. Fejer, S. J. B. Yoo, R. L. Byer, A. Harwit, and J. S. Harris, Phys. Rev. Lett. **62**, 1041 (1989).
[5] Ph. Boucaud, F. H. Julien, D. D. Yang, J.-M. Lourtioz, E. Rosencher, Ph. Bois, and J. Nagle, Appl. Phys. Lett. **57**, 215 (1990).
[6] Jacob B. Khurgin, Greg Sun, Lionel R. Friedman, and R. A. Soref, J. Appl. Phys. **78**, 7398 (1995).
[7] Jacob B. Khurgin and S. Li, Appl. Phys. Lett. **62**, 126 (1993).
[8] N. Vodjani, B. Vinter, V. Berger, E. Bockenhoff, and E. Costard, Appl. Phys. Lett. **59**, 555 (1989).
[9] J. Faist, F. Capasso, D. L. Sivco, A. L. Hutchinson, C. Sirtori, and A. Y. Cho, Science **264**, 553 (1994).
[10] Walter L. Bloss, J. Appl. Phys. **66**, 3639 (1989).
[11] B. Jogai, J. Vac. Sci. Technol. B **9**, 2473 (1991).
[12] Paul Von Allmen, Phys. Rev. B **46**, 13 351 (1992).
[13] Paul Von Allmen, M. Berz, F. K. Reinhart, and G. Harbeke, Semicond. Sci. Technol. **3**, 1211 (1988).
[14] Jerome Faist, Carlo Sitori, Federico Capasso, Loren Pfeizer, and Ken W. West, Appl. Phys. Lett. **64**, 872 (1994).
[15] K. L. Chapman, H. Schmidt, A. Imamoglu, and A. C. Gossard, Appl. Phys. Lett. **69**, 2554 (1996).
[16] E. L. Martinet, H. C. Chui, G. L. Woods, M. M. Fejer, J. S. Harris, C. A. Rella, B. A. Richman, and H. A. Schwettman, Appl. Phys. Lett. **65**, 2630 (1994).
[17] H. C. Chui, G. L. Woods, M. M. Fejer, E. L. Martinet, and J. S. Harris, Jr., Appl. Phys. Lett. **66**, 265 (1995).
[18] Hiromitsu Asai and Yuichi Kawamura, Appl. Phys. Lett. **56**, 746 (1990).
[19] Y. Hirayama, J. H. Smet, L. H. Peng, C. G. Fonstad, and E. P. Ippen, Appl. Phys. Lett. **63**, 1663 (1993).
[20] H. C. Chui and J. S. Harris, Jr., J. Vac. Sci. Technol. B **12**, 1019 (1994).
[21] J. T. Remillard, H. Wang, D. G. Steel, J. Oh, J. Pamulapati, and P. K. Bhattacharya, Phys. Rev. Lett. **62**, 2861 (1989).
[22] D. Gammon, B. V. Shannabrook, and D. S. Katzer, Appl. Phys. Lett. **57**, 2710 (1990).
[23] U. D. Venkateswaran, L. J. Cui, M. M. Li, B. A. Weinstein, K. Elcess, C. G. Fonstad, and C. Mailhiot, Appl. Phys. Lett. **56**, 286 (1990).
[24] Jasprit Singh and K. K. Bajaj, Appl. Phys. Lett. **48**, 1077 (1986).
[25] B. E. Hammons, I. J. Fritz, T. M. Brennan, A. J. Howard, and J. A. Olsen, J. Vac. Sci. Technol. B **11**, 932 (1993).
[26] A. Sacedon, F. Gonzalez-Sanz, E. Calleja, E. Munoz, S. I. Molina, F. J. Pacheco, D. Araujo, R. Garcia, M. Lourenco, Z. Yang, P. Kidd, and D. Dunstan, Appl. Phys. Lett. **66**, 3334 (1995).
[27] D. F. Nelson, R. C. Miller, and D. A. Kleinman, Phys. Rev. B **35**, 7770 (1987).
[28] L. Hedin and B. I. Lundquist, J. Phys. C **4**, 2064 (1971).
[29] D. J. Arent, K. Deneffe, C. Van Hoof, J. De Boeck, and G.

Borghs, J. Appl. Phys. **66**, 1739 (1989).
[30] C. T. Liu, S. Y. Lin, D. C. Tsui, H. Lee, and D. Ackley, Appl. Phys. Lett. **53**, 2510 (1988).
[31] T. Ando, Solid State Commun. **21**, 133 (1977).
[32] C. Weisbuch, R. Dingle, A. C. Gossard, and W. Wiegmann, Solid State Commun. **38**, 709 (1981).
[33] A. Dimoulas, A. Derekis, G. Kyriakdis, and A. Christou, Appl. Surf. Sci. **50**, 353 (1991).
[34] P. Boucaud, F. H. Julien, D. D. Yang, J.-M. Lourtioz, E. Rosencher, and P. Bois, Opt. Lett. **16**, 199 (1991).
[35] Jerome Faist, Carlo Sitori, Federico Capasso, Deborah L. Sivco, Albert L. Hutchinson, Sung Nee G. Chu, and Alfred Y. Cho, Appl. Phys. Lett. **63**, 1354 (1993).
[36] J. Y. Duboz, E. Costard, E. Rosencher, P. Bois, and J. Nagle, J. Appl. Phys. **77**, 6492 (1995).
[37] A. E. Siegman, *Lasers* (University Science Books, Mill Valley, CA, 1986), pp. 168–175.
[38] Sumanth Kaushik and Peter L. Hagelstein, IEEE J. Quantum Electron. **30**, 2547 (1994).
[39] P. W. Smith and T. Hansch, Phys. Rev. Lett. **26**, 740 (1971).
[40] F. Keilmann, Appl. Phys. Lett. **14**, 29 (1977).
[41] Z. Xu, P. M. Fauchet, C. W. Rella, B. A. Richman, H. A. Schwettman, and G. W. Wicks, Phys. Rev. B **51**, 10 631 (1995).
[42] D. J. Newson and A. Kurobe, Appl. Phys. Lett. **53**, 2516 (1988).
[43] M. Zaluzny, J. Appl. Phys. **74**, 4718 (1993).
[44] J. Ducuing and N. Bloembergen, Phys. Rev. **133**, A1493 (1964).
[45] William H. Press, Brian P. Flannery, Saul A. Teukolsky, and William T. Vetterling, *Numerical Recipes* (Cambridge University Press, New York, 1986), pp. 529–538.
[46] F. H. Julien, *Intersubband Transitions in Quantum Wells* (Plenum, New York, 1992), pp. 173–182.
[47] I. Vurgaftman, J. R. Meyer, and L. R. Ram-Mohan, IEEE J. Quantum Electron. **32**, 1334 (1996).